

Published in final edited form as:

Clin Immunol. 2009 September ; 132(3): 371–384. doi:10.1016/j.clim.2009.05.016.

Lung vascular endothelial growth factor expression induces local myeloid dendritic cell activation

Svetlana P. Chapoval^{1,2}, Chun Geun Lee¹, Chuyan Tang¹, Achsah D. Keegan², Lauren Cohn¹, Kim Bottomly^{3,4}, and Jack A. Elias¹

¹Section of Pulmonary and Critical Care Medicine, Department of Internal Medicine, Yale University School of Medicine, 300 Cedar Street, 441-C, TAC, New Haven, CT 06520-8057

²Department of Microbiology and Immunology, Center for Vascular and Inflammatory Diseases, University of Maryland School of Medicine, 800 West Baltimore Street, Baltimore, MD 21201

³Section of Immunobiology, Department of Internal Medicine, Yale University School of Medicine, 300 Cedar Street, 441-C, TAC, New Haven, CT 06520-8057

⁴Wellesley College, 106 Central Street, Wellesley, MA 02481, USA

Abstract

We previously demonstrated that vascular endothelial growth factor (VEGF) expression in the murine lung increases local CD11c⁺ MHCII⁺ DC number and activation. In this study, employing a multicolor flow cytometry, we report increases in both myeloid (mDC) and plasmacytoid (pDC) DC in the lungs of VEGF transgenic (tg) compared to WT mice. Lung pDC from VEGF tg mice exhibited higher levels of activation with increased expression of MHCII and costimulatory molecules. As VEGF tg mice display an asthma-like phenotype and lung mDC play a critical role in asthmatic setting, studies were undertaken to further characterize murine lung mDC. Evaluations of sorted mDC from VEGF tg lungs demonstrated a selective upregulation of cathepsin K, MMP-8, -9, -12, and -14, and chemokine receptors as compared to those obtained from WT control mice. They also had increased VEGFR2 but downregulated VEGFR1 expression. Analysis of chemokine and regulatory cytokine expression in these cells showed an upregulation of macrophage chemotactic protein-3 (MCP-3), thymus-expressed chemokine (TECK), secondary lymphoid organ chemokine (SLC), macrophage-derived chemokine (MDC), IL-1 β , IL-6, IL-12 and IL-13. The antigen (Ag) OVA-FITC uptake by lung DC and the migration of Ag-loaded DC to local lymph nodes were significantly increased in VEGF tg mice compared to WT mice. Thus, VEGF may predispose the lung to inflammation and/or repair by activating local DC. It regulates lung mDC expression of innate immunity effector molecules. The data presented here demonstrate how lung VEGF expression functionally affects local mDC for the transition from the innate response to a Th2-type inflammatory response.

© 2009 Elsevier Inc. All rights reserved.

Correspondence: Svetlana P. Chapoval, Department of Microbiology and Immunology, Center for Vascular and Inflammatory Diseases, University of Maryland School of Medicine, 800 West Baltimore Street, Baltimore, MD 21201; e-mail: schapoval@som.umaryland.edu. Current address: ² Department of Microbiology and Immunology, Center for Vascular and Inflammatory Diseases, University of Maryland School of Medicine, 800 West Baltimore Street, Baltimore, MD 21201; ⁴Wellesley College, 106 Central Street, Wellesley, MA 02481

Publisher's Disclaimer: This is a PDF file of an unedited manuscript that has been accepted for publication. As a service to our customers we are providing this early version of the manuscript. The manuscript will undergo copyediting, typesetting, and review of the resulting proof before it is published in its final citable form. Please note that during the production process errors may be discovered which could affect the content, and all legal disclaimers that apply to the journal pertain.

Keywords

Rodent; lung; inflammation; dendritic cells; cell activation

Introduction

Lung dendritic cells (DC) are critical in controlling the immune response to inhaled antigen (1). In steady state conditions, immature DC are distributed throughout the lung tissue. They constantly sample inhaled Ag and then mature and migrate to the T cell areas of the local lymphoid tissues, peribronchial (mediastinal) lymph nodes. Depending on many factors, including the nature and dose of Ag, the cytokine milieu at the site of Ag entry, lung DC can either stimulate clonal expansion of Ag-specific T cells or induce tolerance. The key role of DC in the interface between tolerance and immune response in the lung is a subject of many investigations (1).

Lung DC are critically modified by many soluble factors such as growth factors, chemokines, and cytokines that are released from different cells within the lung and/or produced by DC themselves. These soluble factors regulate the intensity and duration of immune response to antigen by stimulating or inhibiting activation and function of DC.

One such factor is VEGF.

VEGF, also known as vascular permeability factor, is one of the most important growth and survival factors for endothelium (3). In addition to the induction of endothelial cell proliferation and angiogenesis, lymphangiogenesis, and vasodilatation (2,3), it also stimulates cell migration (4) and inhibits apoptosis (5). VEGF is a heparin-binding glycoprotein that is secreted as a 45 kDa homodimer (2,6) by most types of cells including epithelial cells (7) and T cells (8) with Th2 cells (9) being the prevalent producers. Among several known splice variants of human molecule, VEGF165 is the most abundant (2).

VEGF induces its biological effect through binding to VEGFRs. There are three receptors in the VEGF receptor family named VEGFR1 (fms-like tyrosine kinase-1, Flt-1), VEGFR2 (kinase insert domain-containing receptor/fetal liver kinase-1, KDR/Flk-1), and VEGFR3 (Flt-4) (2). VEGF165 binds to VEGFR1 and 2. VEGFRs were identified on many cell types including DC (2). In addition to VEGFRs, VEGF interacts with a family of co-receptors, the neuropilins (2).

Previous studies of the effect of VEGF on DC activation and function showed controversial results (10–12). VEGF had been reported to inhibit DC development (10), however, the outcome could be dose- (11) and Ag- (12) dependent. The effect of VEGF on lung DC has never been investigated.

We have shown that VEGF positively affects lung DC number and activation (9,13). In the current study, we further investigated the role of VEGF in regulating the immune response in the lung. We examined the effect of VEGF on lung DC subtypes and found an increase in lung mDC and pDC populations. We also studied the role of VEGF in lung mDC basic functions such as the innate immunity sentinel and effector molecule expression, Ag uptake and migration to the lymph nodes. We found that VEGF regulates the mDC expression of chemokines, chemokine receptors, cathepsins, and MMPs. Moreover, VEGF expression augments DC function. In contrast to the previously reported downregulatory effect of VEGF on spleen and skin DC, we show here that lung DC are affected positively by VEGF.

Materials and methods

Mice

The generation and characterization of VEGF tg mice on C57BL/6 background were described in detail previously (9,13). To induce the transgene expression, one month old tg mice were placed on doxycyclin (DOX)-containing water and were evaluated at different time intervals thereafter. DOX-receiving C57BL/6 (WT) mice serve as tg-negative controls. All experiments with the mice were performed in compliance with the principles and procedures outlined in the NIH Guide for Care and Use of Animals and were approved by the Yale University School of Medicine Animal Care and Use Committee.

DC isolation

Two different techniques were used for DC isolation. Where indicated, single cell suspensions from the lungs of WT and VEGF tg mice were prepared by mincing the organs into small pieces and digesting them with type IV collagenase (Worthington Biochemical Corp., Lakewood, NJ) and DNase (Roche, Mannheim, Germany) as described previously (14). RBC were lysed with Ammonium-Chloride-Potassium (K) (chloride), ACK lysis buffer (Invitrogen, Carlsbad, CA) according to the manufacturer's instruction. Otherwise, the digestion step was omitted and the lung single cell suspensions were freshly prepared according to a procedure reported by Piggott DA et al. (15).

Flow cytometry

The staining of lung digest cells for FACS analysis was performed as described elsewhere. The following mAbs obtained from BD Biosciences Pharmingen (San Diego, CA) were used: anti-I-A β^b -biotin (AF6-120.1), anti-CD3-FITC (145-2C11), anti-CD4- phycoerythrin, -PE (GK1.5), anti-CD8 α -PE (53-6.7), anti-CD11b- allophycocyanin-cyanin dye, APC-Cy7 (M1/70), anti-CD11c-FITC or -APC (HL3), anti-CD40-PE (3.23), anti-CD54-PE (3E2), anti-CD80-PE (16-10A1), anti-CD86-PE (GL1), anti-B220/CD45R-PE (RA3-6B2), anti-GR1-FITC or -APC (Ly-6G and Ly-6C). PE-labeled anti-B7h/ICOS-L (HK5.3) Ab was obtained from eBioscience. PE-Cy-5-labeled Mac1 (CD11b/CD18) Ab that were used in some experiments were obtained from Cedarlane Laboratories. DEC-205 was visualized using rat anti-mouse CD205 Ab (NLDC-145) and STAR69 (F(ab')₂ goat anti-rat IgG-FITC), both from Serotec (Oxford, UK). Biotinylated rat anti-mouse F4/80 Ab (CI:A3-1; Serotec) was used in combination with SAV-FITC (BD Pharmingen) for visualization of this macrophage marker. Alexa fluor 647 – labeled anti-CCR7 Ab (4 B12; Biolegend, San Diego, CA) and their isotype control Alexa fluor 647-rat IgG2a, k were used in experiments aimed to analyze CCR7 expression on DC. PE-conjugated rat IgG2a (R35-95) and rat IgG2b (R35-38) were used as isotype controls. Streptavidin-peridinin chlorophyll protein, SAV-PerCP was used as a second step reagent for biotinylated anti-I-A β^b . Where necessary, cells were preincubated with anti-CD16/CD32 (2.4G2) mAb for blocking cell surface FcR. Cells gated by forward- and side-scatter parameters were analyzed on either FACSCalibur or LSRII (Becton Dickinson, San Jose, CA) flow cytometer using either CELLQuest, FACSDiva, or FlowJo softwares. The PI staining was not performed to exclude dead cells in lung digests. Dead cells were eliminated by gating out of cell analysis and cell sort.

Flow cytometry cell sorting

Lung mDC were sorted using either dual or triple marker combination (CD11c/MHCII or CD11c/MHCII/CD11b) employing FACS Vantage, Dako MoFlo, or BD Aria cell sorters at the Yale University School of Medicine Flow Cytometry Core Facility. Autofluorescent macrophages and cell doublets were eliminated from further analysis by proper gating.

Cell morphology

For the studies of sorted cell morphology, 100 μ l of sorted cells were cytopspinned, subjected to Diff-Quik stain (Dade Behring Inc., Newark, DE) and analyzed using Olympus BH-2 microscope. To induce DC maturation, sorted cells were placed on poly-L-lysine-coated slides (Fisher Scientific, Pittsburgh, PA), incubated at 37°C for 30 min and then microscopically analyzed.

In vitro Ag uptake study

Single cell suspension from undigested whole lung tissues were obtained as described above. Lung mDC were sorted using CD11c-APC and MHCII-PE dual markers for identification. Lung cells and sorted mDC were subjected to the *in vitro* cultures with or without increasing doses of OVA-FITC (Molecular Probes, Eugene, OR) ranging from 0.01 mg/ml to 1 mg/ml in RPMI (Life Technologies, Grand Island, NY) in 24-well plates (Costar, Cambridge, MA) for 30 min at 37°C. Cells were plated in either 500,000 or 100,000 cells/well numbers (lung cells or sorted mDC, respectively). After incubation, cells were extensively washed with RPMI medium and analyzed for Ag uptake by flow cytometry. Either 10,000 or 3,000 cells were analyzed in different experiments. Lung cells were stained with CD11c-APC and MHCII-PerCP to analyze the Ag uptake.

In vivo Ag uptake and DC migration study

1 mg/50 μ l/mouse of OVA-FITC was applied *i.n.* to WT and VEGF tg mice one time. Lung tissue and local LN digests were analyzed by flow cytometry 6h and 24h after Ag application for FITC+ cells using CD11c/MHCII/CD11b markers. In addition, 100 μ l of cells were used for the cytospin and following fluorescent microscopy evaluation.

Immunohistochemistry

Lungs from WT and VEGF tg mice were inflated with 4% OCT embedding medium (Electron Microscopy Sciences, Fort Washington, PA) and embedded to this compound in freezing chambers over 2-methyl butane (Sigma) by slowly freezing on liquid nitrogen. Cryostat cut frozen tissue sections were mounted on poly-L-lysine-coated slides (Fisher Scientific, Pittsburgh, PA) and stored at -70°C until stained. Endogenous peroxidase activity was blocked using 3% H₂O₂ and 0.1% NaN₃ (Sigma) for 5 min. Nonspecific binding was prevented by preincubation of the slides with 10% goat serum (Biomed Corporation, Foster City, CA) for 30 min. The specific Ab staining was performed according to the technical data sheets provided. To identify the marker-positive cells in the lung tissue, primary Ab to either CD11c (BD Pharmingen) or DEC-205 (NLDC-145; Cedarlane Laboratories, Hornby, Ontario, Canada) were used in working dilution 1:50. CD11c-positive staining was visualized via three-step staining procedure using biotinylated anti-hamster cocktail (BD Pharmingen) as the secondary Ab and Streptavidin-HRP (Abcam Inc., Cambridge, MA) as the detection enzyme. For DEC-205 staining visualization, HRP goat anti-rat IgG (Cedarlane Laboratories) was used. All incubation steps lasted 30 min. Aminoethylcarbazole (Sigma) substrate solution was used for the HRP reaction development. RT-PCR and real-time RT-PCR

Sorted mDC were washed in medium at 1200 rpm for 5 min at 40°C. Total RNA (tRNA) was extracted from cell pellet using TRIzol reagent (Invitrogen Life Technologies, Carlsbad, CA) and chloroform isolation procedure combined with the RNeasy mini kit (Qiagen, Valencia, CA) according to manufacturer's instruction. One μ g of tRNA was transcribed into first strand cDNA using SuperScript kit (Invitrogen Life Technologies, Carlsbad, CA). Then 500 ng of cDNA was used for PCR amplification. PCR reaction products were run on 1.5% agarose gels and visualized using ethidium bromide. Real-time RT-PCR with tRNA samples was performed using Quanti-Test SYBR Green RT-PCR Master Kit (Qiagen) using either Smart Cycler II

System (Cepheid) or ABI Sequence Detection System (Applied Biosystem). Quantification of the target gene expression was done by comparison with the expression of β -actin. The gene specific primers for RT-PCR and real time RT-PCR were designed using the Primer3 Input 0.4.0 software. The amplicon specificity was verified by gel running and/or by sequencing.

Western blot

Sorted lung mDC were washed in medium as described above. Cell pellets were subjected to 200 μ l of protein lysis buffer (16) for 15 min at 4°C. Then, the suspension was spun down at 3000 rpm for 5 min. Supernatants were collected and total protein concentrations were measured using Bradford method (Bio-Rad kit). For the initial optimization experiments, 5, 10, 15, and 20 μ g of denatured protein were used for protein loading, subsequent transferring to nitrocellulose membrane, specific staining for β -tubulin, and visualization as described (24). In the following experiments, 15 μ g of total protein was used with the corresponding 1:200 diluted primary Abs, all purchased from Santa Cruz Biotechnology: IL-1 β (M-20, sc-1251), MMP-12 (M-19, sc-8839), MMP-9 (C-20, sc-6840), and macrophage inflammatory protein-1 α , MIP-1 α (M-20, sc-1383), MIP-1 β (M-20, sc-1387), and donkey anti-goat IgG-HRP (sc-2020, dilution 1:1000) as the secondary Ab. Biotinylated anti-CCR5 Ab (C34-3448, BDBiosciences) were used in combination with Streptavidin-horse radish peroxidase (HRP) (Abcam Inc., Cambridge, MA).

Statistics

Cell count data were summarized as mean \pm SEM. To calculate significance levels between experimental groups, Student's t test (Microsoft Excel) was performed. Significant differences between groups were established when $p \leq 0.05$.

Results

Lung VEGF expression increases local numbers of CD11c⁺ and DEC-205⁺ cells We have reported previously that VEGF expression alters the lung DC number and activation (9,13). To study DC localization in the lung, we performed immunostaining with anti-CD11c Ab and found a significant increase in CD11c⁺ cells in the lung sections obtained from VEGF tg mice compared to WT mice (Figure 1A). CD11c⁺ cells are distributed throughout the lung tissue. As CD11c molecule could be expressed by other cell types in the lung (17), we performed tissue immunolabeling with anti-DEC-205 Ab (Figure 1B). DEC-205 is expressed on immature lung DC and its expression increases with cell maturation (18,19). We observed a significant increase in both the number and brightness of DEC-205⁺ cells in the lung tissue sections obtained from VEGF tg mice compared to WT counterparts (Figure 1B, C). Therefore, VEGF increases the number of lung DC and their expression levels of DEC-205.

Lung VEGF expression increases local numbers of both myeloid and plasmacytoid DC

It has been shown that more than 95% of lung DC in naïve WT mice are of an immature myeloid phenotype being CD11c⁺MHCII^{low} CD11b⁺ (17,19,20). As expected, mDC in the lungs of naïve WT mice were CD11c⁺MHCII⁺ (Figure 2A). They expressed low levels of F4/80 and CD11b, indicating that they were not macrophages (Figure 2B). In VEGF tg mice, we observed upregulation of MHCII and CD11b expression, as we previously described (9,13). In addition, mDC level of DEC-205 was increased whereas the level of F4/80 was downregulated by tg expression.

pDC in the lung of WT mice are CD11c^{intermed}/B220⁺/GR1⁺ (Figure 2C) as defined previously (21). More than 50% of CD11c^{intermed}/GR1⁺ cells co-express B220/CD45R (Figure 2B) (21). This number increases in VEGF tg pDC to more than 70%. VEGF expression induces

activation of these cells as they upregulate MHCII, CD40, CD80, CD86, and CD54 expression on their surface without a substantial modulation of ICOS-L expression.

Morphology of lung DC

In order to avoid a non-specific DC activation, lung mDC were isolated with omitting an enzymatic digestion step (15). There are several subpopulations of CD11c⁺ cells in WT lungs distinguished by the level of CD11c and MHCII expression (Figure 3). Both CD11c⁺MHCII^{neg} and CD11c⁺MHCII^{low} cells can represent either different subtypes of lung mDC based on their lung tissue localization or different stages of maturation of the same lung mDC subtype. There was a shift to CD11c⁺MHCII^{high} population in VEGF tg lungs which also increased in cell numbers compared to CD11c⁺MHCII^{low} population in WT counterparts. These cells (gate R2) were selected for sorting and further analysis. Lungs from VEGF tg mice also showed an increase in CD11c^{intermed/high}MHCII^{high} cells (gate R4) that exhibited a granulocyte morphology.

VEGF affects chemokine receptor, chemokine, and cytokine expressions in lung mDC

To study if VEGF has an effect on lung mDC chemokine receptor expression, we analyzed mRNA levels for selected specific receptors by RT-PCR (Figure 4A) and real-time RT-PCR in sorted cells (Figure 4B). DC from VEGF tg mice exhibit increased mRNA expression of most of the chemokines receptors. Upregulation of CCR1, CCR2, and CCR5 was especially prominent, whereas the expression of CCR4 and CCR6 was either low or undetectable in these cells. Lung mDC from VEGF tg mice also exhibited increased CCR5 and CCR7 protein level (Figure 4C, D). Therefore, VEGF overexpression in the lung induces an upregulation of specific chemokine receptors on lung mDC which are characteristics of both immature and mature DC (22, 23). We next examined if lung mDC from VEGF tg mice had altered chemokine expression. We observed strong stimulation of the mRNA accumulation representing MCP-3, TECK, SLC, and MDC (Figure 4A) in VEGF tg lung mDC. Neither MIP-1 α nor MIP-1 β protein was detected in mDC (data not shown).

We then studied the VEGF expression-induced cytokine dysregulation in lung mDC. VEGF tg mouse mDC demonstrated a marked upregulation in IL-1 β and IL-13 and an induction of IL-12 and IL-15 (Figure 4A, C). IL-6 expression was also upregulated in these cells as compared to WT counterparts. IFN- α , - β , - γ , IL-4, -5, -9, and -10 were not detected (data not shown).

VEGF regulates specific cathepsins and MMPs in lung DC

Specific cathepsins and MMPs are critical for DC migration, maturation, and activation (24, 25) therefore critically affecting their basic functions. Lung VEGF expression leads to a strong upregulation of mRNA encoding cathepsin K in mDC and only marginally affects the expression of other cathepsins (Figure 5A). At the same time, it has no effect on cathepsin S expression on either mRNA or protein levels (Figure 5A, B). Whereas expression of MMP-8, -9, -12, and -14 were highly upregulated by VEGF, MMP-2 and -7 were low or undetectable (Figure 5A, B). VEGF regulates VEGF receptor complex expression in lung DC

It has been shown previously that under certain conditions VEGF might have an inhibitory effect on DC (26,10) which could be mediated by VEGFR1 but not by VEGFR2 (27,28). Therefore we examined the VEGFR complex expression on mDC obtained from WT and VEGF tg mouse lungs. We found that VEGF exposure induces mRNA expression of VEGFR2 and downregulates VEGFR1 in lung mDC (Figure 5A). In addition, VEGF upregulates both VEGF co-receptors, neuropilin-1 and -2.

Increased in vitro Ag uptake by lung DC obtained from VEGF tg mice

To investigate the impact of the in vivo VEGF expression on the in vitro Ag uptake by DC, sorted lung mDC were cultured in vitro with or without increasing concentrations of OVA-FITC as described in Materials and Methods section. VEGF tg mDC are significantly more efficient in Ag uptake with low doses of Ag used (Figure 6). For example, at 10 μ g of Ag only 30.2 % of WT DC were FITC+ whereas for VEGF tg DC this number increased to 73.9%. At high dose both WT and tg mDC are equally efficient in Ag uptake.

Increased in vivo Ag uptake by lung DC in VEGF tg mice

To investigate the impact of VEGF expression on in vivo lung DC function, we used i.n. application of OVA-FITC to mice. Fluorescent microscopic examination of lung cells revealed an increased number of FITC+ cells in VEGF tg mice compared to WT mice at 6h and 24 h after Ag application (Figure 7A–B). In addition, an obvious increase in Ag uptake per individual lung APC was observed. We observed an increase in FITC+ DC but not Mac-1+ cell number in VEGF tg lungs by flow cytometry (Figure 7C). Therefore, intermediately mature mDC obtained from the lung of VEGF tg mice are more efficient in Ag uptake.

Augmented migration of activated APC into local lymph nodes in VEGF tg mice

To study the effect of lung VEGF expression on the migration of OVA-FITC-loaded DC into local LN, we performed both fluorescent microscopic and flow cytometric evaluation of LN tissue digests. We have found an increase in FITC+ cell numbers in the LN of VEGF tg mice at 6h and 24h after OVA-FITC i.n. application compared to WT mice (Figure 8A, B). These data were confirmed using flow cytometry analysis (Figure 8C). Whereas the numbers of FITC+ cells in WT LN were 6.0 ± 0.4 % and 13.3 ± 0.4 % at 6h and 24h after Ag application, correspondingly, for VEGF tg mice these numbers mounted to 17.8 ± 0.9 and 32.2 ± 0.6 , 6 and 24 h, correspondingly ($p < 0.00035$, FITC+ cells among draining LN cells, WT vs tg mice).

Discussion

Previously, we have shown that the inducible expression of VEGF by lung epithelial cells (9, 13), secreted and present in the lung tissue at physiologic (29) levels (≥ 0.1 ng/ml) had a stimulatory effect on local DC increasing their number and activation stage based on MHCII and costimulatory molecule expression. In this work, for the first time, we provide more detailed evidence how lung VEGF expression affects local DC populations, their activation state and function.

VEGF is generated by most tumors including lung cancer (30). The VEGF-induced DC dysfunction was proposed to be one of the mechanisms by which tumors escape immune recognition (10,26,27). The fact that VEGF has a contrasting effect in asthma and tumor, on pulmonary and non-pulmonary DC could have several possible explanations. First of all, in cancer patients and in animal models of tumor there is already an immunosuppressive environment (31) that itself affects DC status and possibly modulates their VEGFR expression (32). The other explanation is that bone marrow-, lymphoid tissue-, or peripheral blood-derived DC are different from lung DC. Although this requires further detailed examination, it is currently known that the lung lacks CD8+ DC under steady state conditions (1,21,33) but these cells are readily being detected in lymphoid tissues and peripheral blood (34,35). Currently, there are six reported mouse lymphoid tissue DC subclasses, namely CD4+, CD8+, CD4+CD8+ and CD4-CD8- DC (subdivided on at least two subpopulations) and pDC (35). Previously, two lung DC populations were clearly distinguished, mDC and pDC (1,21,33,36). Currently, there are three reported mouse lung tissue DC subclasses, namely CD11b+ mDC, pDC, and CD103+ mDC (37–39). The in vitro adherence cultures of lung mature CD8- DC were reported to give a rise to CD8+ DC (19). To clarify the DC population that is being affected by lung

VEGF expression, we performed analysis of lung cell suspensions for mDC and pDC using corresponding markers (Figure 2). We did not use CD103 marker to define the third lung DC population at this time. Lung VEGF expression induces the increases in both local DC populations, mDC and pDC. It is an especially interesting observation as it has been shown that these two DC populations display opposing functions in the experimental lung asthmatic conditions (21,36,40). Whereas lung mDC are absolutely required for both acute and chronic asthmatic responses (36,40) by initiating and promoting asthmatic conditions, lung pDC play a downregulatory role in this setting by inducing regulatory T cells (21). This could be explained, in part, by their higher expression of ICOS-L (18, Figure 2B). Interestingly, increases in both mDC and pDC in the airways of asthmatic patients have been reported previously (41) suggesting that both DC subpopulations are affected by allergen exposure and the consequences of such.

Previous studies have demonstrated that continuous long term VEGF infusions lead to the dysfunction and abnormal differentiation of DC (10). Furthermore, the methods of cytokine delivery to the mice have different effects on DC. The use of recombinant VEGF is unpractical as it quickly disappears from circulation and does not show any significant effect on DC (10). Interestingly, the use of a pump infusion method for the external VEGF delivery to the mice led not only to DC downregulation but also to a dramatic sequestration of lymph node tissue with GR1+ cells with eosinophilic morphology (10). This observation further supports our conclusion that VEGF itself induces and promotes Th2 responses.

The nature of the Ag and the local cytokine milieu can modify VEGF effects on DC. A direct effect of VEGF on DC in cultures was demonstrated using human monocyte-derived DC (12). These cells were generated with IL-4 plus GM-CSF and then matured with either LPS or a proinflammatory cytokine cocktail (TNF α , IL-1 β , IL-6 and PGE2) in the presence or absence of increasing doses of recombinant VEGF. When DC maturation was induced by LPS, VEGF addition to the cultures led to the down-regulation of costimulatory molecules and the induction of apoptosis. In contrast, in DC matured by proinflammatory cytokines, no such effect was seen. The authors also demonstrated the downregulation of VEGFR-2/Flk-1 expression with DC maturation although they did not specify if LPS and proinflammatory cytokine cocktail similarly affect VEGFRs. In addition, the VEGFR expression can be differently regulated on different DC subsets by different stimuli including VEGF itself. For example, VEGF binds VEGFR1/Flt-1 expressed on hematopoietic progenitor cells and blocks activation and transcription of NF- κ B in these cells (42) leading to their apoptosis. The downregulatory effect of VEGF on the *in vitro* embryonic stem cell differentiation into DC was mediated by VEGFR1 but not by VEGFR2 (30). Moreover, VEGFR2 was found to be critical for DC differentiation as its disruption dramatically decreased DC number (27). We show here that pulmonary mDC express VEGFR1 but not VEGFR2 (Figure 5A, B). Interestingly, VEGF expression induced lung mDC activation and the simultaneous downregulation of their expression of inhibitory VEGFR1 and induction, at least on mRNA level, of stimulatory VEGFR2.

We also show here that lung VEGF expression leads to the intermediate activation of lung mDC based on the expression pattern of their costimulatory molecules (9,13), chemokines (Figure 4A) and chemokine receptors (Figure 4A–D). While selected costimulatory molecule expression on lung DC have been a subject of several studies (9,13,15,35,36,43), there is only a scarce number of reports about chemokines, chemokine receptors, and other innate immunity sentinel and effector molecules regulation in lung DC.

Several *in vitro* studies have shown that immature DC produce inflammatory chemokines CXCL8 (IL-8), CXCL10 (interferon-inducible protein 10, IP-10), CCL3 (MIP-1 α), CCL4 (MIP-1 β), and CCL5 (Regulated on Activation, Normal T Expressed and Secreted chemokine, RANTES) (23). Upon maturation, DC lose the ability to produce these chemokines and

generate T- and B-cell chemoattractants CCL17 (thymus and activation-regulated chemokine, TARC), CCL18 (DC-CK1), CCL19 (MIP-3 β), and CCL22 (MDC). On the other hand, it has been shown previously that Th2-promoting DC express MCP, TARC, and secondary lymphoid organ chemokine, SLC while Th1 promoting DC express RANTES, MIP-1 α , and MIP-1 β (44,45). Therefore, mDC in VEGF tg lungs are more Th2-promoting (Figure 4). CD11b⁺ and CD103⁺ lung mDC populations were reported to be different in their chemokine production in both homeostasis and inflammation (38) for the latter being a higher producer of Th2-promoting chemokines TARC and MDC. The regulation CD103 expression on lung mDC by VEGF remains to be determined. In addition, it has been shown that IL-12-secreting DC together with external source of IFN γ from NK cells or memory T cells prime strong Th1 response, while IL-6-secreting DC together with an external source of IL-4 prime strong Th2 response (1,46). Our data on IL-6 expression by WT lung mDC (Figure 4A) further support previous observations that lung mDC are preferential inducers of Th2 response and require an obligatory signal to induce Th1 immunity (1,43). Our data on upregulation of IL-6 and IL-13 in tg lung mDC (Figure 4A) further support our hypothesis that VEGF generates Th2-promoting lung environment through its specific action on lung DC.

Chemokine receptors expression is used as one of the characteristics to distinguish immature and mature DC (22,23). Immature DC in the blood and nonpulmonary tissues express so called “proinflammatory” chemokine receptors such as CCR1, CCR2, CCR5, CCR6 and also CXCR1, CXCR2, and CXCR4 (22,23). However, studies on DC in other tissues can not be extrapolated to lung DC as they are morphologically and functionally different. To this date, there are two incomplete reports on chemokine receptor expression on lung DC (20,47). In one report, Swanson KA and colleagues have shown that lung immature DC express various low levels of CCR1, CCR2, CCR5, CCR6, and CCR7 (19). Mature DC population differed from immature DC by increased expression of CCR2, CCR5 and CCR6. In other report, Chiu BC and colleagues have shown that lung DC express measurable amounts of mRNA for CCR1, CCR5, and CXCR4 while the expression of CCR2, CCR4, CCR6, CCR7, and CXCR3 was not found (47). We show here that WT lung sorted mDC have low levels of CCR1, CCR2, CCR7, CXCR2, and CXCR4 expression (Figure 4A). Expression of CCR3, CCR4, CCR5, CCR6, and CCR8 was not detected. VEGF expression upregulates lung mDC expression of CCR1, CCR2, CCR7, CXCR2, and CXCR4, and induces CCR3, CCR5, and CCR8 (Figure 4A, B, C, and D). This study supports our conclusion that lung mDC in VEGF tg mice are in the intermediate activation stage as, in addition to intermediate upregulation of costimulatory molecule expressions (9), they also demonstrated upregulation of CC and CXC chemokine receptors that are found in both, immature and mature DC. In addition, upregulation of CCR7 which is a specific receptor for secondary lymphoid chemokine (SLC) and MIP-3 β might, in part, explain the observed enhanced migration of lung DC into the local lymph nodes in tg mice after OVA-FITC inhalation (Figure 8). Both these chemokines are constitutively expressed in afferent lymphatics and T cell area of lymph node (1,22,48).

Multiple extracellular matrix degrading proteases can be upregulated and activated in DC during their migration from the blood to the lung and from the lung to the local lymph nodes. As the role of specific cathepsins in antigen processing and presentation is well established, their role in DC migration and activation is not. Multiple extracellular matrix degrading enzymes can be upregulated and activated in DC along their migration track from the blood to the lung and from the lung to the local lymph nodes. All cathepsins are able to cleave, degrade, remodel, and process extracellular matrix (49). It is known that upon DC maturation cysteine protease activity is increased (24). We show here that lung VEGF expression leads to a strong upregulation of mRNA for cathepsins K and only marginally affects the expression of other cathepsins (Figure 5). Based on our observation it is likely that mDC-derived cathepsin K is involved in mDC migration in tg mice.

MMPs play a role in the migration and maturation of DC (25,50). The migration of Langerhans cells and skin DC to lymph nodes was inhibited by broad spectrum MMP inhibitor BB-3103, or by Abs to MMP-2 and MMP-9, or by administration of natural tissue inhibitors of MMPs, tissue inhibitor of matrix metalloproteases 1 and 2, TIMP-1 and TIMP-2 suggesting critical roles of these MMPs in regulating DC migration (50). Moreover, in MMP-9 KO mice no such migration was observed, however DC maturation and their ability to stimulate T cells were intact. Interestingly, MMP-9 KO mice demonstrated significantly diminished airway inflammation, local IL-13 production, and AHR because of a defective DC migration into the airways leading to decreased levels of DC-derived Th2-attracting chemokines (25). We show here that VEGF expression leads to the induction of MMP-9, -12, and -14 in lung mDC and upregulation of MMP-8 (Figure 5A, B). It remains critical to determine the role of cathepsins and MMPs in DC function in order to effectively manipulate it to specifically treat or prevent allergic asthmatic disease.

It is well established that fully mature lung mDC express high surface levels of MHCII and costimulatory molecules. Some Ag (43), cytokines (51) and other factors (17) can lead to full DC maturation. However, certain combination of agents induces only partial lung DC activation (9,52). This intermediately mature DC are unable to induce stimulation of T cells (52). It remains to be determined if VEGF-exposed intermediately mature lung mDC are the effective T cell proliferation/cytokine production stimulators. However, the fact that we observe an asthma-like phenotype in VEGF tg mice and the reported exaggerated response of VEGF tg mice to OVA (9) let us to hypothesize that these DC could be effective inducers of a Th2-type response. Indeed, these intermediately mature mDC display Th2-promoting phenotype based on their cytokines and chemokines expressions.

For the first time, we provide here a characteristic of WT lung mDC expression of chemokines, chemokine receptors, cytokines, cathepsins, and MMPs. This is also first observation of how VEGF affects lung mDC function. The fact that VEGF is upregulated in asthma patients (53) provides a further proof of importance of VEGF regulation as a therapeutic strategy for asthma and other Th2 mediated disorders.

Supplementary Material

Refer to Web version on PubMed Central for supplementary material.

Acknowledgments

The authors thank Bart N. Lambrecht (Department of Pulmonary and Critical Care Medicine, Erasmus University Medical Center, Rotterdam, Netherlands) for his helpful suggestions and comments for this work. The authors thank Gouzel Tokmoulina and Yale University School of Medicine Cell Sorter Facility staff for help with cell cytometry and sorting.

This work was supported by the National Institute of Health grants HL-64242, HL-78744, HL-66571, HL-56389 awarded to Jack A. Elias.

References

1. Vermaelen K, Pauwels R. Pulmonary dendritic cells. *Am J Respir Critic Care Medicine* 2005;172:530–551.
2. Ferrara N, Gerber HP, LeCouter J. The biology of VEGF and its receptors. *Nat Med* 2003;9:669–676. [PubMed: 12778165]
3. Nagy JA, Vasile E, Feng D, Sundberg C, Brown LF, Detmar MJ, Lawitts JA, Benjamin L, Tan X, Manseau EJ, Dvorak AM, Dvorak HF. Vascular permeability factor/vascular endothelial growth factor induces lymphangiogenesis as well as angiogenesis. *J Exp Med* 2002;196:1497–1506. [PubMed: 12461084]

4. Heil M, Clauss M, Suzuki K, Buschmann IR, Willuweit A, Fischer S, Schaper W. Vascular endothelial growth factor (VEGF) stimulates monocyte migration through endothelial monolayers via increased integrin expression. *Eur J Cell Biol* 2000;79:850–857. [PubMed: 11139149]
5. Kasahara Y, Tuder RM, Taraseviciene-Stewart L, Le Cras TD, Abman S, Hirth PK, Waltenberger J, Voelkel NF. Inhibition of VEGF receptors causes lung cell apoptosis and emphysema. *J Clin Invest* 2000;106:1311–1319. [PubMed: 11104784]
6. Houck KA, Leung DW, Rowland AM, Winer J, Ferrara N. Dual regulation of vascular endothelial growth factor bioavailability by genetic and proteolytic mechanisms. *J Biol Chem* 1992;267:26031–26037. [PubMed: 1464614]
7. Koyama S, Sato E, Tsukadaira A, Haniuda M, Numanami H, Kurai M, Nagai S, Izumi T. Vascular endothelial growth factor mRNA and protein expression in airway epithelial cell lines in vitro. *Eur Respir J* 2002;20:1449–1456. [PubMed: 12503703]
8. Heslan JM, Branellec A, Laurent J, Lagrue G. The vascular permeability factor is a T lymphocyte product. *Nephron* 1986;42:187–188. [PubMed: 3484808]
9. Lee CG, Link H, Baluk P, Homer RJ, Chapoval S, Bhandari V, Kang MJ, Cohn L, Kim YK, McDonald DM, Elias JA. Vascular endothelial growth factor (VEGF) induces remodeling and enhances TH2-mediated sensitization and inflammation in the lung. *Nat Med* 2004;10:1095–1103. [PubMed: 15378055]
10. Gabrilovich D, Ishida T, Oyama T, Ran S, Kravtsov V, Nadaf S, Carbone DP. Vascular endothelial growth factor inhibits the development of dendritic cells and dramatically affects the differentiation of multiple hematopoietic lineages in vivo. *Blood* 1998;92:4150–4166. [PubMed: 9834220]
11. Kim BG, Lee JH, Yi SY, Woo HJ, Yun YS. Overexpression of VEGF in MOPC 315 plasmacytoma enhances antitumor cytotoxic T lymphocyte response [abstract]. *Cancer Detection & Prevention*. 2000
12. Takahashi A, Kono K, Ichihara F, Sugai H, Fujii H, Matsumoto Y. Vascular endothelial growth factor inhibits maturation of dendritic cells induced by lipopolysaccharide, but not by proinflammatory cytokines. *Cancer Immunol Immunother* 2004;53:543–550. [PubMed: 14666382]
13. Bhandari V, Choo-Wing R, Chapoval SP, Lee CG, Tang C, Kim YK, Ma B, Baluk P, Lin MI, McDonald DM, Homer RJ, Sessa WC, Elias JA. Essential role of nitric oxide in VEGF-induced, asthma-like angiogenic, inflammatory, mucus, and physiologic responses in the lung. *Proc Natl Acad Sci U S A* 2006;103:11021–11026. [PubMed: 16832062]
14. Niu N, Le Goff MK, Li F, Rahman M, Homer RJ, Cohn L. A novel pathway that regulates inflammatory disease in the respiratory tract. *J Immunol* 2007;178:3846–3855. [PubMed: 17339484]
15. Piggott DA, Eisenbarth SC, Xu L, Constant SL, Huleatt JW, Herrick CA, Bottomly K. MyD88-dependent induction of allergic Th2 responses to intranasal antigen. *J Clin Invest* 2005;115:459–467. [PubMed: 15650773]
16. Lee PJ, Zhang X, Shan P, Ma B, Lee CG, Homer RJ, Zhu Z, Rincon M, Mossman BT, Elias JA. ERK1/2 mitogen-activated protein kinase selectively mediates IL-13-induced lung inflammation and remodeling in vivo. *J Clin Invest* 2006;116:163–173. [PubMed: 16374521]
17. Maraskovsky E, Brasel K, Teepe M, Roux ER, Lyman SD, Shortman K, McKenna HJ. Dramatic increase in the numbers of functionally mature dendritic cells in Flt3 ligand-treated mice: multiple dendritic cell subpopulations identified. *J Exp Med* 1996;184:1953–1962. [PubMed: 8920882]
18. Vermaelen KY, Carro-Muino I, Lambrecht BN, Pauwels RA. Specific migratory dendritic cells rapidly transport antigen from the airways to the thoracic lymph nodes. *J Exp Med* 2001;193:51–60. [PubMed: 11136820]
19. Swanson KA, Zheng Y, Heidler KM, Zhang ZD, Webb TJ, Wilkes DS. Flt3-ligand, IL-4, GM-CSF, and adherence-mediated isolation of murine lung dendritic cells: assessment of isolation technique on phenotype and function. *J Immunol* 2004;173:4875–4881. [PubMed: 15470028]
20. Vermaelen K, Pauwels R. Accurate and simple discrimination of mouse pulmonary dendritic cell and macrophage populations by flow cytometry: methodology and new insights. *Cytometry* 2004;61:170–177. [PubMed: 15382026]
21. de Neer HJ, Hammad H, Soullie T, Hijdra D, Vos N, Willart MAM, Hoogsteden HC, Lambrecht BN. Essential role of lung plasmacytoid dendritic cells in preventing asthmatic reactions to harmless inhaled antigen. *J Exp Med* 2004;200:89–98. [PubMed: 15238608]

22. Sallusto F, Lanzavecchia A. Understanding dendritic cell and T-lymphocyte traffic through the analysis of chemokine receptor expression. *Immunol Rev* 2000;177:134–140. [PubMed: 11138771]
23. McColl SR. Chemokines and dendritic cells: a crucial alliance. *Immunol Cell Biol* 2002;80:489–496. [PubMed: 12225386]
24. Trombetta ES, Ebersold M, Garrett W, Pypaert M, Mellman I. Activation of lysosomal function during dendritic cell maturation. *Science* 2003;299:1400–1403. [PubMed: 12610307]
25. Vermaelen KY, Cataldo D, Tournoy K, Maes T, Dhulst A, Louis R, Foidart JM, Noël A, Pauwels R. Matrix metalloproteinase-9-mediated dendritic cell recruitment into the airways is a critical step in a mouse model of asthma. *J Immunol* 2003;171:1016–1022. [PubMed: 12847275]
26. Ishida T, Oyama T, Carbone DP, Gabrilovich DI. Defective function of Langerhans cells in tumor-bearing animals is the result of defective maturation from hemopoietic progenitors. *J Immunol* 1998;161:4842–4851. [PubMed: 9794417]
27. Dikov MM, Ohm JE, Ray N, Tchekneva EE, Burlison J, Moghanaki D, Nadaf S, Carbone DP. Differential roles of vascular endothelial growth factor receptors 1 and 2 in dendritic cell differentiation. *J Immunol* 2005;174:215–222. [PubMed: 15611243]
28. Meyer RD, Mohammadi M, Rahimi N. A single amino acid substitution in the activation loop defines the decoy characteristic of VEGFR-1/FLT-1. *J Biol Chem* 2006;281:867–875. [PubMed: 16286478]
29. Simcock DE, Kanabar V, Clarke GW, O'connor BJ, Lee TH, Hirst SJ. Proangiogenic activity in bronchoalveolar lavage fluid from patients with asthma. *Am J Respir Crit Care Med* 2007;176:146–153. [PubMed: 17463417]
30. Voelkel NF, Vandivier RW, Tuder RM. Vascular endothelial growth factor in the lung. *Am J Physiol Lung Cell Mol Physiol* 2006;290:L209–L221. [PubMed: 16403941]
31. Frumento G, Piazza T, Di Carlo E, Ferrini S. Targeting tumor-related immunosuppression for cancer immunotherapy. *Endocr Metab Immune Disord Drug Targets* 2006;6:233–237. [PubMed: 17017974]
32. Breier G, Blum S, Peli J, Groot M, Wild C, Risau W, Reichmann E. Transforming growth factor-beta and Ras regulate the VEGF/VEGF-receptor system during tumor angiogenesis. *Int J Cancer* 2002;97:142–148. [PubMed: 11774256]
33. van Rijt LS, Jung S, KleinJan A, Vos N, Willart M, Duez C, Hoogsteden HC, Lambrecht BN. In vivo depletion of lung CD11c+ dendritic cells during allergen challenge abrogates the characteristic features of asthma. *J Exp Med* 2005;201:981–991. [PubMed: 15781587]
34. Vremec D, Zorbas M, Scollay R, Saunders DJ, Ardavin CF, Wu L, Shortman K. The surface phenotype of dendritic cells purified from mouse thymus and spleen: investigation of the CD8 expression by a subpopulation of dendritic cells. *J Exp Med* 1992;176:47–58. [PubMed: 1613465]
35. Edwards AD, Chaussabel D, Tomlinson S, Schulz O, Sher A, Reis e Sousa C. Relationships among murine CD11c(high) dendritic cell subsets as revealed by baseline gene expression patterns. *J Immunol* 2003;171:47–60. [PubMed: 12816982]
36. Lambrecht BN, De Veerman M, Coyle AJ, Gutierrez-Ramos JC, Thielemans K, Pauwels RA. Myeloid dendritic cells induce Th2 responses to inhaled antigen, leading to eosinophilic airway inflammation. *J Clin Invest* 2000;106:551–559. [PubMed: 10953030]
37. Sung SS, Fu SM, Rose CE Jr, Gaskin F, Ju ST, Beaty SR. A major lung CD103 (alphaE)-beta7 integrin-positive epithelial dendritic cell population expressing Langerin and tight junction proteins. *J Immunol* 2006;176:2161–2172. [PubMed: 16455972]
38. Beaty SR, Rose CE Jr, Sung SS. Diverse and potent chemokine production by lung CD11bhigh dendritic cells in homeostasis and in allergic lung inflammation. *J Immunol* 2007;178:1882–1895. [PubMed: 17237439]
39. Jakubzick C, Tacke F, Ginhoux F, Wagers AJ, van Rooijen N, Mack M, Merad M, Randolph GJ. Blood monocyte subsets differentially give rise to CD103+ and CD103- pulmonary dendritic cell populations. *J Immunol* 2008;180:3019–3027. [PubMed: 18292524]
40. Lambrecht BN, Salomon B, Klatzmann D, Pauwels RA. Dendritic cells are required for the development of chronic eosinophilic airway inflammation in response to inhaled antigen in sensitized mice. *J Immunol* 1998;160:4090–4097. [PubMed: 9558120]
41. Bratke K, Lommatzsch M, Julius P, Kuepper M, Kleine HD, Luttmann W, Christian Virchow J. Dendritic cell subsets in human bronchoalveolar lavage fluid after segmental allergen challenge. *Thorax* 2007;62:168–175. [PubMed: 16928719]

42. Oyama T, Ran S, Ishida T, Nadaf S, Kerr L, Carbone DP, Gabrilovich DI. Vascular endothelial growth factor affects dendritic cell maturation through the inhibition of nuclear factor-kappa B activation in hemopoietic progenitor cells. *J Immunol* 1998;160:1224–1232. [PubMed: 9570538]
43. Stumbles PA, Thomas JA, Pimm CL, Lee PT, Venaile TJ, Proksch S, Holt PG. Resting respiratory tract dendritic cells preferentially stimulate T helper cell type 2 (Th2) responses and require obligatory cytokine signals for induction of Th1 immunity. *J Exp Med* 1998;188:2019–2031. [PubMed: 9841916]
44. Vissers JL, Hartgers FC, Lindhout E, Teunissen MB, Figdor CG, Adema GJ. Quantitative analysis of chemokine expression by dendritic cell subsets in vitro and in vivo. *J Leukoc Biol* 2001;69:785–793. [PubMed: 11358988]
45. Sallusto F, Lanzavecchia A, Mackay CR. Chemokines and chemokine receptors in T-cell priming and Th1/Th2-mediated responses. *Immunol Today* 1998;19:568–574. [PubMed: 9864948]
46. Dodge IL, Carr MW, Cernadas M, Brenner MB. IL-6 production by pulmonary dendritic cells impedes Th1 immune responses. *J Immunol* 2003;170:4457–4464. [PubMed: 12707321]
47. Chiu BC, Freeman CM, Stolberg VR, Hu JS, Zeibecoglou K, Lu B, Gerard C, Charo IF, Lira SA, Chensue SW. Impaired lung dendritic cell activation in CCR2 knockout mice. *Am J Pathol* 2004;165:1199–1209. [PubMed: 15466386]
48. Randolph GJ. Dendritic cell migration to lymph nodes: cytokines, chemokines, and lipid mediators. *Semin Immunol* 2001;13:267–274. [PubMed: 11502161]
49. Bühling F, Waldburg N, Reisenauer A, Heimburg A, Golpon H, Welte T. Lysosomal cysteine proteases in the lung: role in protein processing and immunoregulation. *Eur Respir J* 2004;23:620–628. [PubMed: 15083765]
50. Ratzinger G, Stoitzner P, Ebner S, Lutz MB, Layton GT, Rainer C, Senior RM, Shipley JM, Fritsch P, Schuler G, Romani N. Matrix metalloproteinases 9 and 2 are necessary for the migration of Langerhans cells and dermal dendritic cells from human and murine skin. *J Immunol* 2002;168:4361–4371. [PubMed: 11970978]
51. Feili-Hariri M, Falkner DH, Morel PA. Polarization of naive T cells into Th1 or Th2 by distinct cytokine-driven murine dendritic cell populations: implications for immunotherapy. *J Leukoc Biol* 2005;78:656–664. [PubMed: 15961574]
52. Sporri R, Reis e Sousa C. Inflammatory mediators are insufficient for full dendritic cell activation and promote expansion of CD4⁺ T cell populations lacking helper function. *Nat Immunol* 2005;6:163–170. [PubMed: 15654341]
53. Hoshino M, Nakamura Y, Hamid QA. Gene expression of vascular endothelial growth factor and its receptors and angiogenesis in bronchial asthma. *J Allergy Clin Immunol* 2001;107:1034–1038. [PubMed: 11398081]

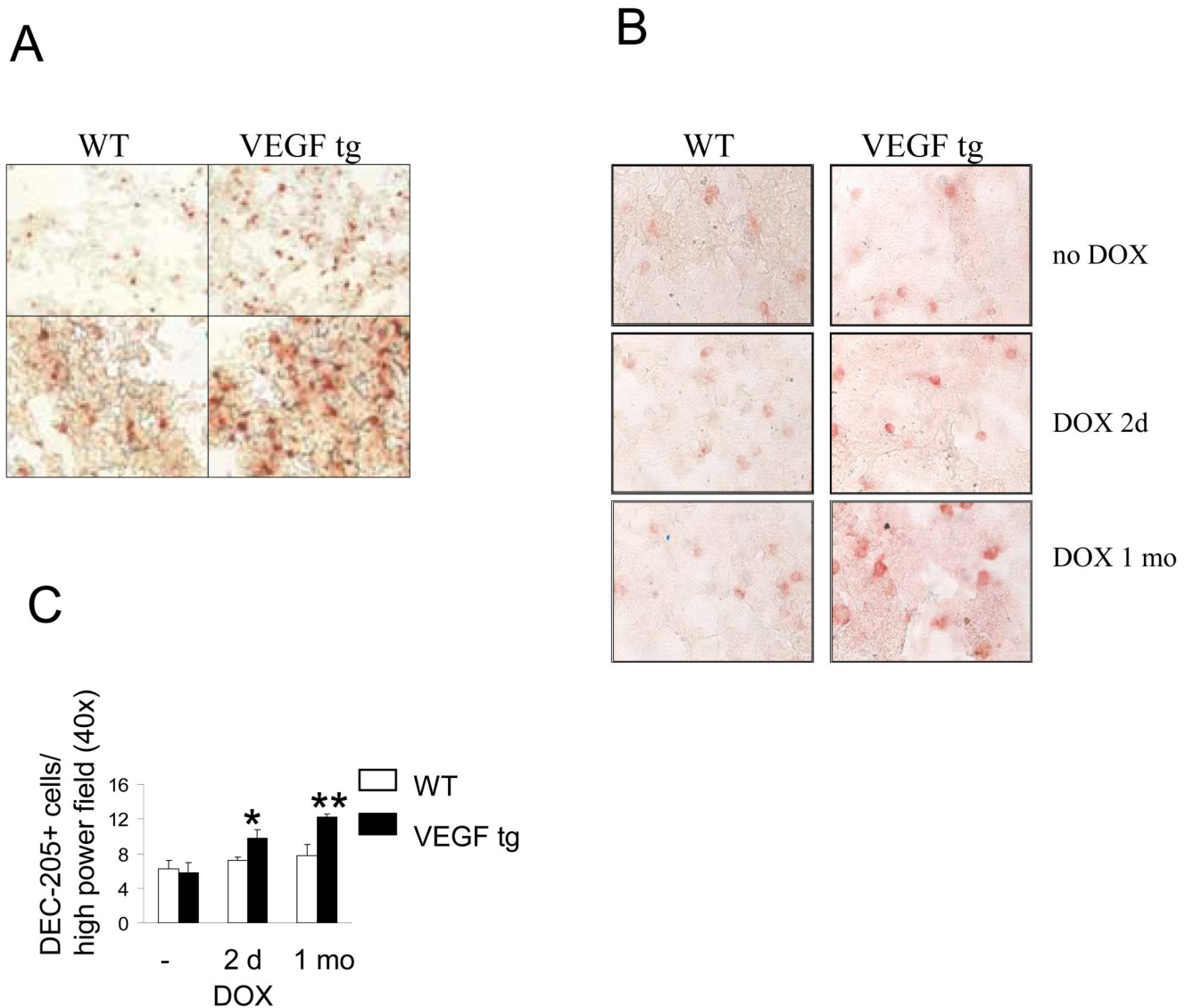


Figure 1. Lung VEGF expression increases the numbers of CD11c+ (A) and DEC-205+ (B–C) cells in tg mouse lungs. Mouse lung frozen tissue was processed and stained with appropriate Ab as described in Materials and Methods. (A) Magnification correspondingly: upper panel – 10 \times , lower panel – 40 \times . (B) Magnification 40 \times . (C) Marker-positive cells were counted in minimum 4 fields. * p <0.03 and ** p <0.0027, VEGF tg mice vs WT counterparts, n =3 per group.

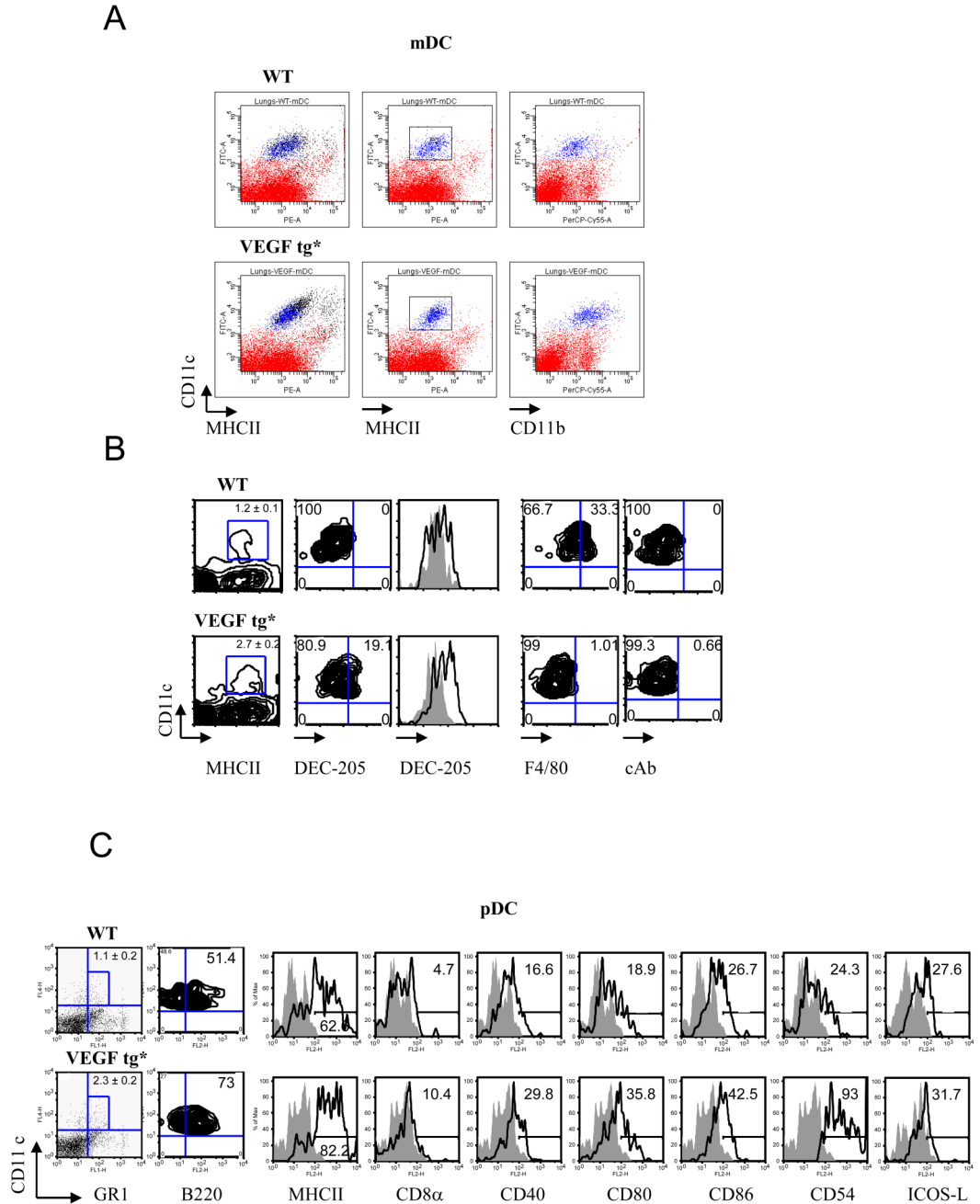


Figure 2. Lung VEGF expression increases the number and activation of myeloid (A, B) and plasmacytoid (C) DC in tg mouse lung. Mouse lung tissues were obtained on day 7 of DOX water administration and processed as described in Materials and Methods. Single cell suspensions were stained with corresponding Ab and analyzed by flow cytometry. The results shown represent individual mouse in one out of three experiments. (A–B) Autofluorescent macrophages (shown in black color in panel A) were removed from the DC analysis. An upregulation of MHCII, CD11b, DEC-205 but not F4/80 expression on tg lung mDC was detected. For histograms: solid line represents isotype control rat IgG2a staining whereas transparent line shows the level of DEC-205 expression. *p<0.0025, WT vs tg lung mDC

number (n=5/group). (C) Mouse lung pDC number increases in VEGF tg mice as compared to WT counterparts (1.1 ± 0.2 vs 2.3 ± 0.2 , correspondingly, n=6, p<0045). Autofluorescent macrophages and mDC (CD11^{high}) were gated out of this analysis. Histograms demonstrate upregulation of selected markers on lung pDC in VEGF tg mice.

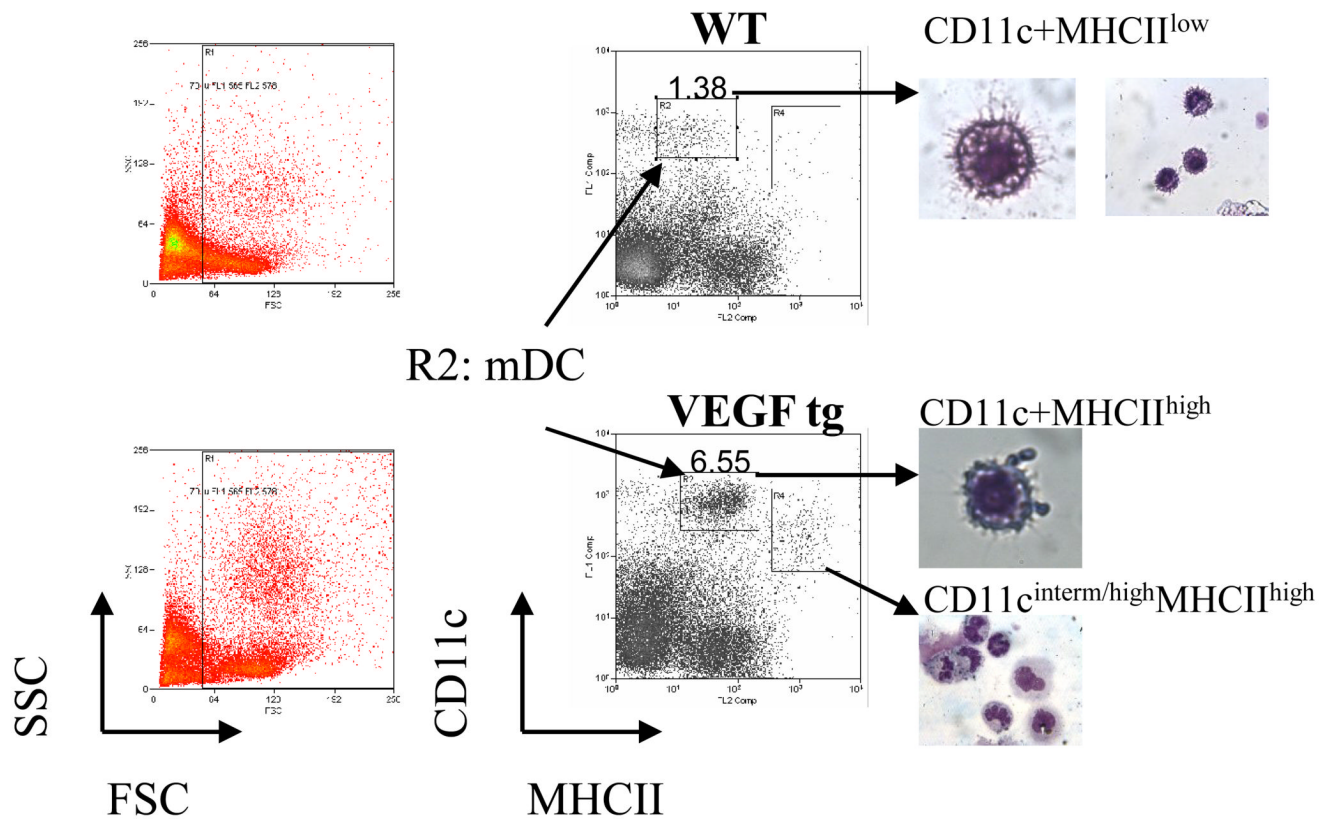


Figure 3.

Sorted lung mDC acquisition and morphology. Single cell suspensions from WT and VEGF tg mouse lungs (n=4–5 mice per experiment) prepared with omitting enzymatic digestion step were stained with α -CD11c and α -MHCII Ab, analyzed using either CellQuest, FACSDiva, or Summit software on cells sorters, and then assigned cell populations were sorted and analyzed morphologically as described in Materials and Methods. The sorted mDC selected for further characterization represent CD11c+MHCII^{low} population of cells in WT mice and CD11c+MHCII^{high} population in VEGF tg mice (gate R2). CD11c^{interm/high}MHCII^{high} cells in gate R4 displayed a granulocyte-like morphology.

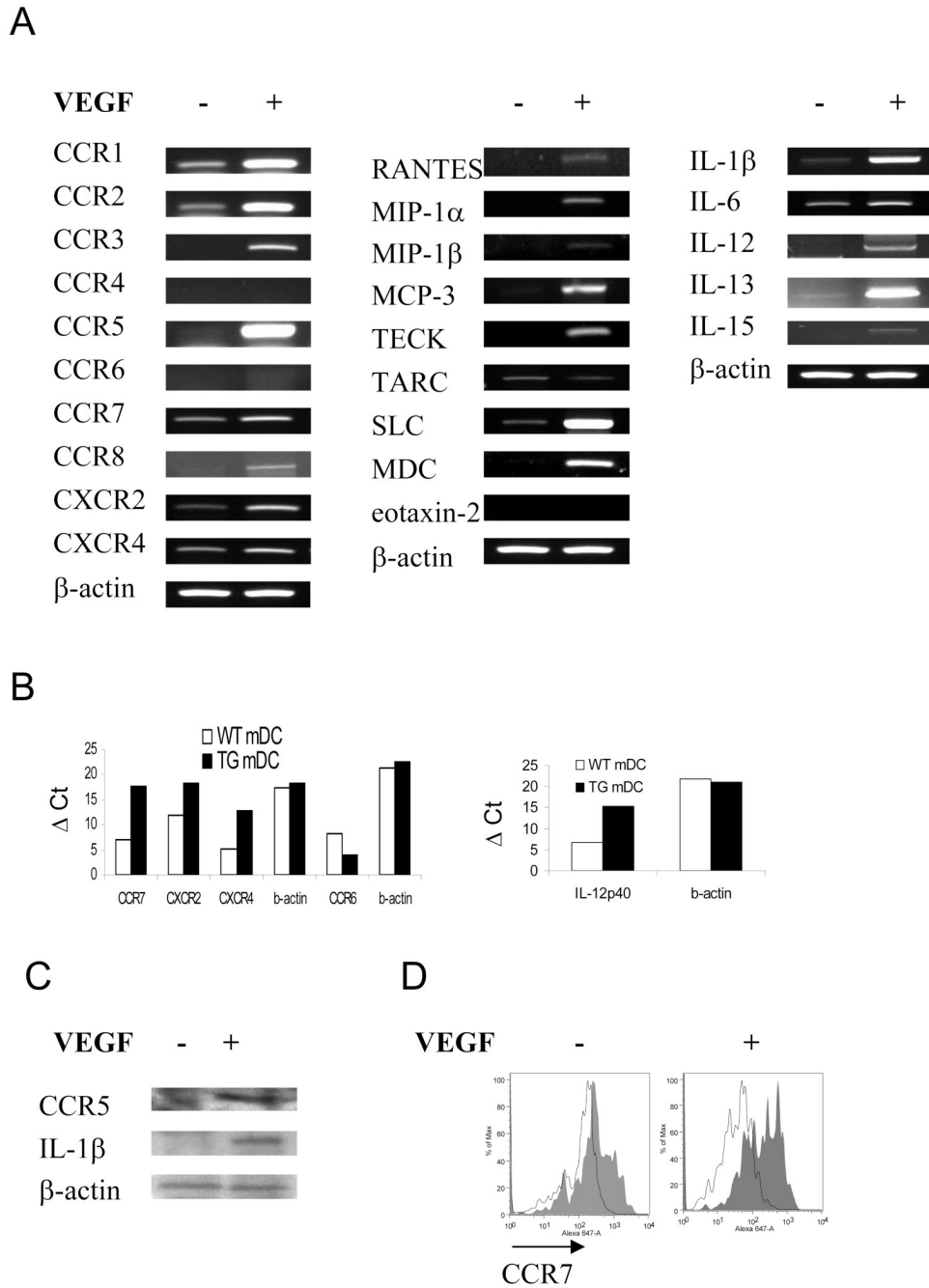


Figure 4. VEGF regulates the expression of specific chemokine receptors (A–D), chemokines (A), and cytokines (A–C) in lung mDC. (A, B) cDNA from sorted lung mDC was obtained as described in Materials and Methods and analyzed for the selected markers using PCR with corresponding primer’s set. Lung VEGF expression regulated local mDC expression of selected chemokine receptors, chemokines, and regulatory cytokines. (B) Upregulation of IL-12p40 expression in tg lung mDC as analyzed by a quantitative real time RT-PCR. (C) Sorted lung mDC were subjected to a protein lysis buffer. Fifteen μg of cellular protein were subjected to a Western blot analysis. Lung VEGF expression induced an upregulation in CCR5 and IL-1β expression in lung mDC. (D) Increased expression of CCR7 (solid line over transparent line which shows

rat IgG2a isotype control stain) on sorted lung mDC obtained from VEGF tg mice as compared to WT cell marker expression analyzed by flow cytometry. (A–D) Mice were placed on DOX water for 7 days.

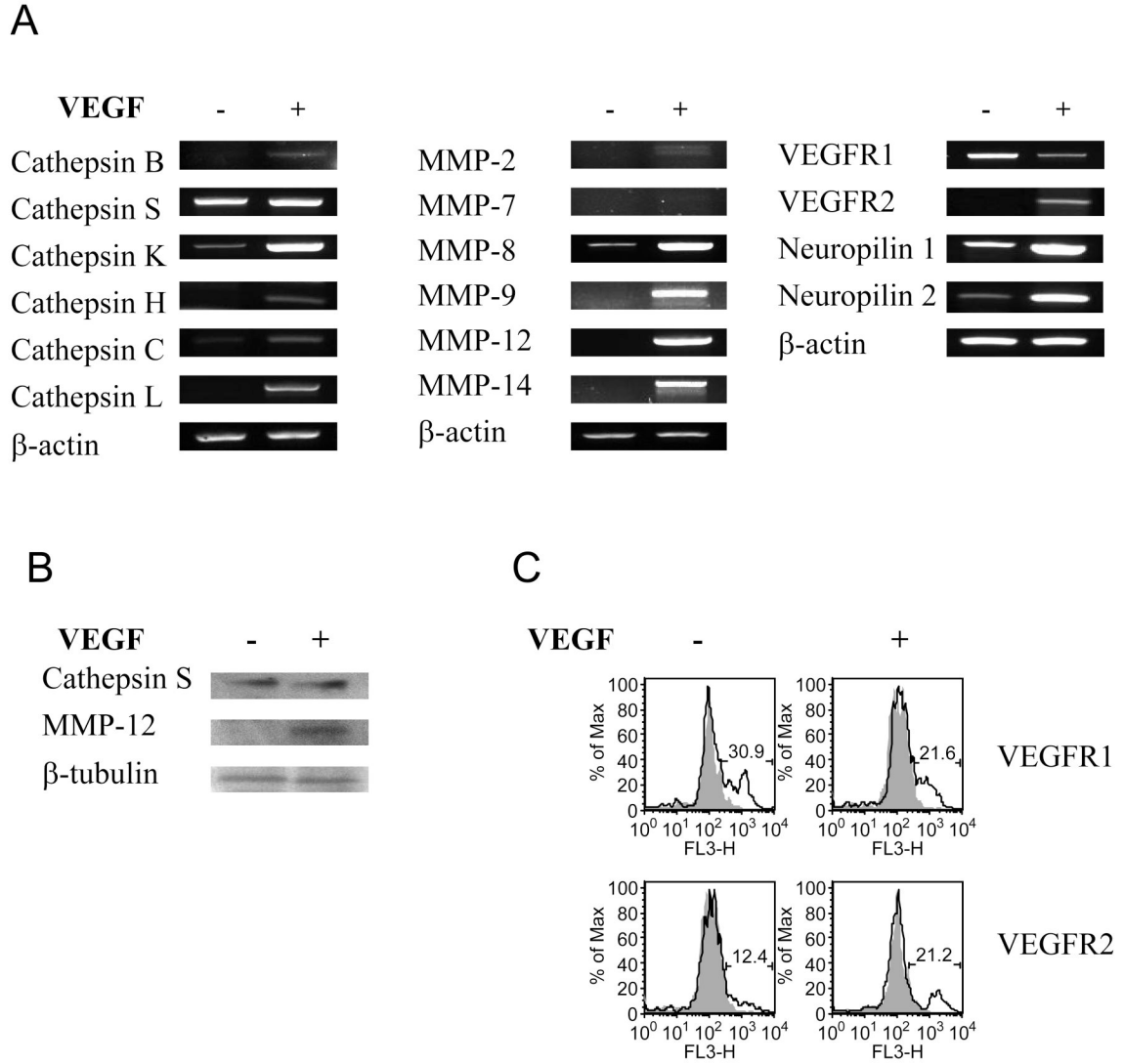


Figure 5. VEGF regulates the expression of specific cathepsins (A, B), MMPs (A, B), and VEGF receptor complex (A) in lung mDC. Sorted lung mDC were subjected to tRNA and following cDNA isolation for PCR (A) as described in Material and Methods with corresponding primer's set. (A) VEGF expression downregulates VEGFR1 and induces VEGFR2 expression in lung mDC. In addition, it upregulates the expression of both neuropilins. (B) VEGF induces MMP-12 but not cathepsin S upregulation in tg mDC as analyzed by Western blot. Of note, cathepsin S is the most highly expressed cathepsin in WT lung mDC.

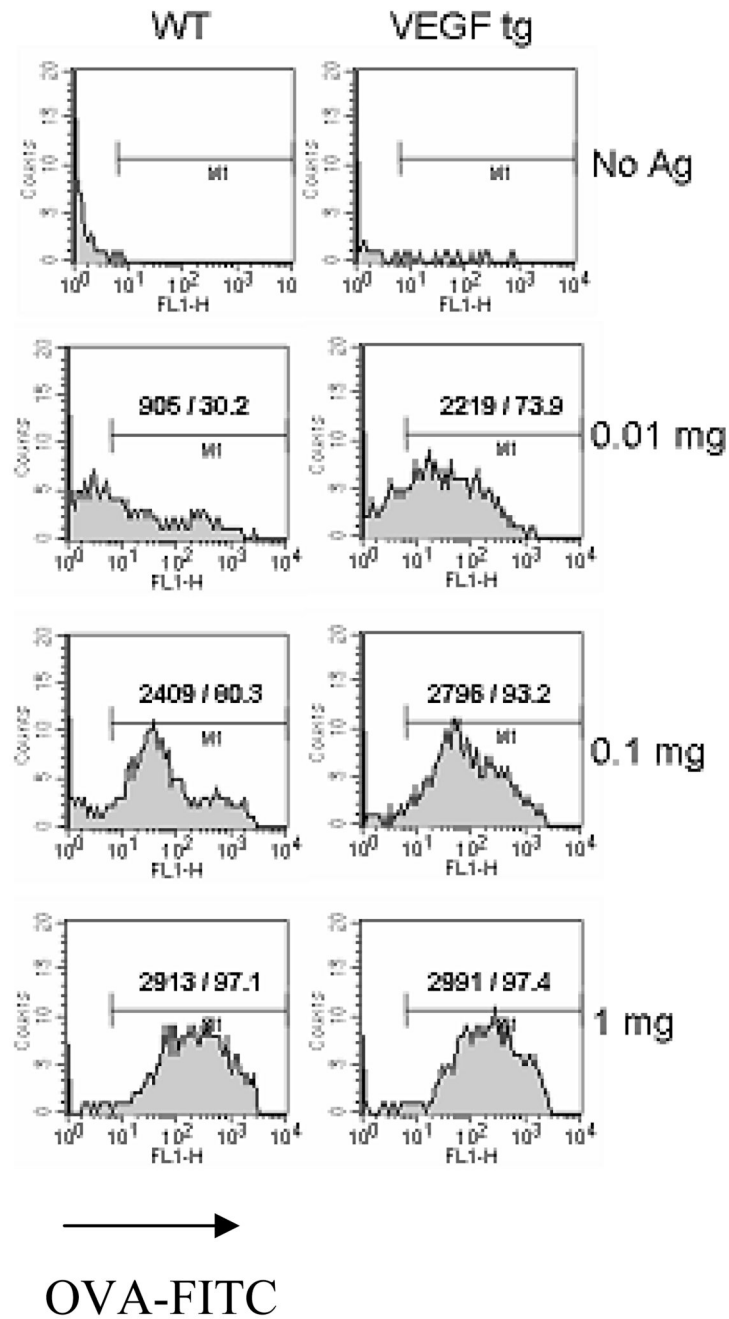


Figure 6.

VEGF-induced increase of in vitro Ag uptake by lung mDC. Lung mDC were sorted using CD11c and MHCII marker expression and subjected to the in vitro cultures with or without OVA-FITC as described in Materials and Methods. Cells were further analyzed by flow cytometry. The shown are absolute and relative numbers of FITC+ mDC among 3000 analyzed cells for each setting in one out of two experiments. Note an increased VEGF tg mDC ability to uptake OVA-FITC at low Ag doses.

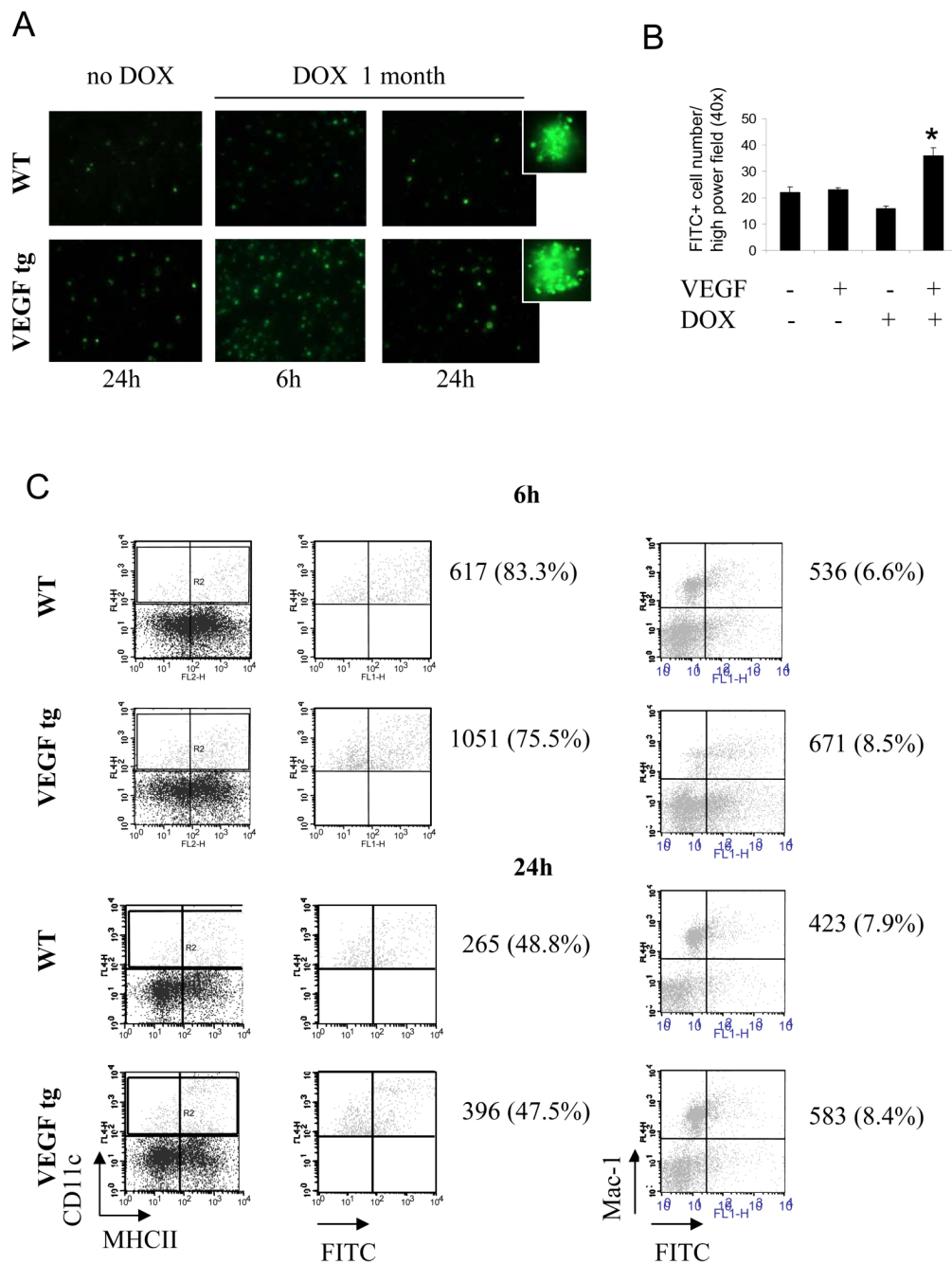


Figure 7. VEGF-induced increase of in vivo Ag uptake by lung DC but not by Mac-1+ macrophages (A–C). WT and VEGF tg mice were kept on either normal or DOX-containing water. OVA-FITC was applied i.n. as described in Materials and Method. Single cell suspensions from lung tissues were analyzed for FITC-positivity by either fluorescent microscopy of cytopinned cells (A–B) or flow cytometry (C), n=2 mice/group/experiment in 3 separate experiments. (A) Fluorescent photomicrographs taken from WT and VEGF tg lung cells at 6h and 24h after intranasal OVA-FITC application. (B) *p<0.004, tg vs WT mice on DOX, p<0.022, tg mice on DOX vs WT and tg without DOX. (C) Lung DC (gate R2) were re-gated on OVA-FITC+.

Shown is the percentage of OVA-FITC+ cells among the gated lung DC (left panel) and the percentage of CD11c-Mac-1+OVA-FITC+ cells (right panel).

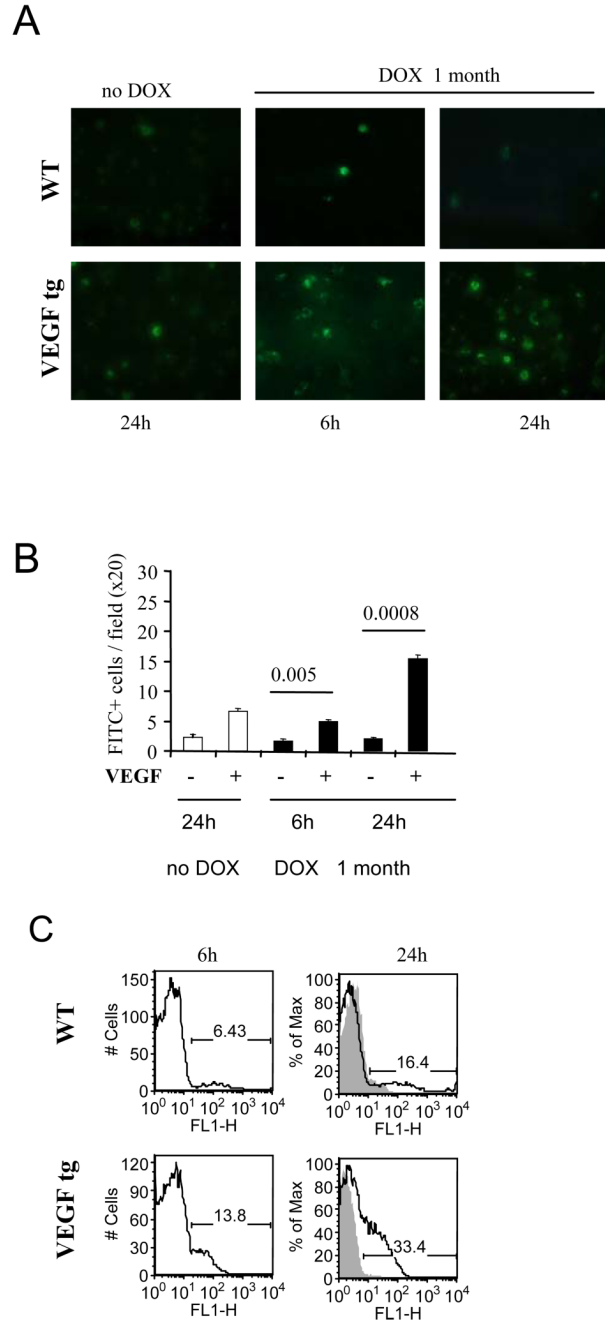


Figure 8. VEGF-induced increase in the in vivo Ag transport by lung DC. The preexisting conditions for the experiments were as described in Figure 7 legends. Single cell suspensions from local lymph nodes were analyzed for FITC-positivity by either fluorescent microscopy of cytospinned cells (A–B) or flow cytometry (C). The results from one out of 3 representative experiments are shown. n=2 mice/group/experiment in 3 separate experiments. Fluorescent photomicrographs taken from WT and VEGF tg lymph node cells at 6h and 24h after intranasal OVA-FITC application (A) and FITC+ cells were enumerated (B). (C) The histograms show the percentage of OVA-FITC+ lymph node cells in the lung of OVA-FITC immunized mice

(clear histogram) as compared to PBS-treated mice (gray histogram) at 6h and 24h after Ag (PBS) application.